

Semiclassical trajectories in the double-slit experiment

Hector H. Hernandez Hernandez*, Carlos R. Javier Valdez†

Universidad Autonoma de Chihuahua, Facultad de Ingenieria, Nuevo Campus
Universitario, Chihuahua 31125, Mexico

June 8, 2021

Abstract

We provide a semiclassical description of the double-slit experiment based on momentous quantum mechanics, where the implementation of canonical variables facilitate the derivation of the equations of motion for the system. We show the evolution of individual particles and their semiclassical trajectories, collectively reproduce the well-known quantum interference pattern. It is found that the non-crossing rule for trajectories, present in Bohmian mechanics, is not required under our treatment. We are able to follow classical configuration variables from this semiclassical scheme, and discuss substantial differences between our description and the Bohmian perspective.

Keywords: Semiclassical quantum mechanics. Double-slit experiment.

PACS: 03.65.Sq, 03.65.w, 03.65.Xp

1 Introduction

One of the most prominent phenomenon in modern physics is the double-slit experiment because it alone shows most of the important features of quantum mechanics, such as the wave-particle duality, wave function collapse, existence of non locality, a way to verify the Born-rule, on different setups [1–5]. These features can be explained within the quantum mechanics framework. However, there are some classical properties, such as the time of flight of the particles that cross through the double slit, that standard quantum mechanics cannot explain or compute by the corresponding expectation value [6]. Standard quantum mechanics lacks a particle-like description, in the classical sense, and so there exist alternative proposals or interpretations [7, 8], being Bohmian mechanics the most complete [9]. In spite of the great concordance that Bohmian mechanics has with standard quantum mechanics, it presents important differences, such as the existence of particle trajectories evolving and interacting with a quantum potential [10], or the interpretation of the superposition principle [11–13]. These differences, however, have implications in the interpretation of the results on the double-slit experiment, such as the reality of trajectories [14].

In this paper we study the double-slit experiment under a semiclassical approach, where we obtain the well-known interference pattern, as well as particle trajectories. These semiclassical trajectories are constrained due to the uncertainty relation of variables on an extended phase space, being in more concordance with the usual interpretation of quantum mechanics. This semiclassical approach is based on an extension of Ehrenfest’s theorem [15–18] and has been successfully employed to study systems such as quantum tunneling, quantum pendulum and quantum cosmology [17–20].

2 Effective dynamics of quantum systems: general definition

The dynamics of expectation values of observables in quantum systems can be described by employing the momentous formulation of quantum mechanics. In this scheme, the evolution of the system is obtained by means of a set of effective equations for expectation values of observables and their associated momenta,

*hernandez@uach.mx

†a310861@uach.mx

allowing us to understand how the classical dynamics of the system is corrected by including quantum effects.

The effective equations of motion are obtained by evaluating Poisson brackets between variables and the quantum corrected Hamiltonian, $\dot{f} = \{f, H_Q\}$, where H_Q is the classical Hamiltonian plus quantum corrections. Expectation values of position, momentum and quantum dispersions are considered classical variables. Expectation values of dispersions and momenta are defined by

$$G^{a,b} := \langle (\hat{x} - x)^a (\hat{p} - p)^b \rangle_{\text{Weyl}}, \quad a + b \geq 2, \quad (1)$$

whereas the quantum corrected Hamiltonian reads

$$\langle \hat{H} \rangle := H_Q = H(x, p) + \sum_{a,b} \frac{1}{a!b!} \frac{\partial^{a+b} H}{\partial x^a \partial p^b} G^{a,b} \quad (2)$$

where $x := \langle \hat{x} \rangle$, $p := \langle \hat{p} \rangle$, and the operators are Weyl ordered. Usual quantum fluctuations can be directly identified: $\Delta x^2 = G^{2,0}$ and $\Delta p^2 = G^{0,2}$.

In general, an infinite number of coupled equations is obtained from (2), providing a complete description of the quantum system. Recently, it was obtained a generalization of this effective method in terms of explicitly canonical variables (s, p_s, U) [17]

$$s = \sqrt{G^{2,0}}, \quad p_s = \frac{G^{1,1}}{\sqrt{G^{2,0}}} \quad (3)$$

$$U = G^{2,0} G^{0,2} - (G^{1,1})^2 \quad (4)$$

In terms of these variables the Hamiltonian (2) can be rewritten as

$$H_Q = \frac{p_x^2 + p_s^2}{2m} + V(x) + \frac{U}{2ms^2} + \sum_a \frac{1}{a!} \frac{\partial^a V}{\partial x^a} G^{a,0} \quad (5)$$

or in a more compact form

$$H_Q = \frac{p_x^2 + p_s^2}{2m} + \frac{U}{2ms^2} + \frac{1}{2} (V(x+s) + V(x-s)). \quad (6)$$

The extension to several degrees of freedom can be obtained in a similar way, with a generalization of (1)

$$G^{a_1, b_1, \dots, a_k, b_k} := \langle (\hat{x}_1 - x_1)^{a_1} (\hat{p}_1 - p_1)^{b_1} \dots (\hat{x}_k - x_k)^{a_k} (\hat{p}_k - p_k)^{b_k} \rangle_{\text{Weyl}} \quad (7)$$

where $a_i + b_i \geq 2$. In this case the general quantum-corrected Hamiltonian is

$$H_Q := \sum_{a_1, b_1}^{\infty} \dots \sum_{a_k, b_k}^{\infty} \frac{1}{a_1! b_1! \dots a_k! b_k!} \frac{\partial^{a_1 + b_1 + \dots + a_k + b_k} H}{\partial x_1^{a_1} \partial p_1^{b_1} \dots \partial x_k^{a_k} \partial p_k^{b_k}} G^{a_1, b_1, \dots, a_k, b_k} \quad (8)$$

3 Effective quantum Hamiltonian for the double-slit experiment

The configuration for the double-slit experiment consists of the following: a source of particles, such as electrons, atoms, etc., a double slit placed in front of it, and a screen that records the position of particles that reach it.

We use the double-slit potential function shown in Fig. 1, introduced in [21]

$$V(x, y) = \left(V_o - \frac{1}{2} m \omega^2 y^2 + \frac{m^2 \omega^4 y^4}{16 V_o} \right) e^{-(x/\alpha)^2} \quad (9)$$

The trajectories of the particles are confined to the xy-plane, thus we set $k = 2$ in the general quantum corrected Hamiltonian (10)

$$\begin{aligned} H_Q = & \frac{p_x^2}{2m} + \frac{p_y^2}{2m} + \frac{1}{2m} G^{0,2,0,0} + \frac{1}{2m} G^{0,0,0,2} + V(x, y) + \sum_{a_2=2}^{\infty} \frac{1}{a_2!} \frac{\partial^{a_2} V(x, y)}{\partial y_2^{a_2}} G^{0,0,a_2,0} \\ & + \sum_{a_1=2}^{\infty} \frac{1}{a_1!} \frac{\partial^{a_1} V(x, y)}{\partial x_1^{a_1}} G^{a_1,0,0,0} \end{aligned} \quad (10)$$

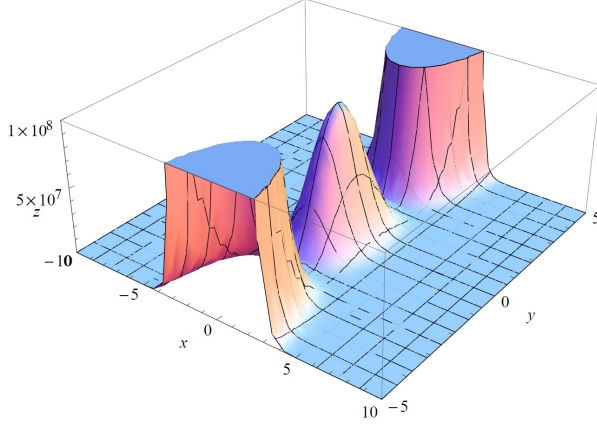


Figure 1: Double slit-potential with $m = 1$, $\omega = 10000$, $V_o = 10^7$ and $\alpha = 1.5$.

In terms of canonical variables the Hamiltonian reads

$$H_Q = \frac{p_x^2 + p_{sx}^2}{2m} + \frac{p_y^2 + p_{sy}^2}{2m} + \frac{U}{2ms_x^2} + \frac{U}{2ms_y^2} + \frac{1}{4} \sum_{i,j=1}^2 V(x + (-1)^i s_x, y + (-1)^j s_y) \quad (11)$$

The corresponding equations of motion are

$$\begin{aligned} \dot{x} &= \frac{p_x}{m}, & \dot{s}_x &= \frac{p_{sx}}{m}, \\ \dot{y} &= \frac{p_y}{m}, & \dot{s}_y &= \frac{p_{sy}}{m}, \\ \dot{p}_x &= \frac{1}{2\alpha^2} \left(2V_o - m\omega^2(y^2 + s_y^2) + \frac{m^2\omega^4}{8V_o} (y^4 + 6y^2s_y^2 + s_y^4) \right) \left((x - s_x)e^{-(\frac{x-s_x}{\alpha})^2} + (x + s_x)e^{-(\frac{x+s_x}{\alpha})^2} \right), \\ \dot{p}_{sx} &= \frac{U}{ms_x^3} + \frac{1}{2\alpha^2} \left(2V_o - m\omega^2(y^2 + s_y^2) + \frac{m^2\omega^4}{8V_o} (y^4 + 6y^2s_y^2 + s_y^4) \right) \left((x + s_x)e^{-(\frac{x+s_x}{\alpha})^2} - (x - s_x)e^{-(\frac{x-s_x}{\alpha})^2} \right), \\ \dot{p}_y &= \left(\frac{m\omega^2 y}{2} - \frac{m^2\omega^4}{8V_o} (s_y^3 + 3ys_y^2) \right) \left(e^{-(\frac{x+s_x}{\alpha})^2} + e^{-(\frac{x-s_x}{\alpha})^2} \right), \\ \dot{p}_{sy} &= \frac{U}{ms_y^3} + \left(\frac{m\omega^2 s_y}{2} - \frac{m^2\omega^4}{8V_o} (s_y^3 + 3y^2s_y) \right) \left(e^{-(\frac{x+s_x}{\alpha})^2} + e^{-(\frac{x-s_x}{\alpha})^2} \right) \end{aligned} \quad (12)$$

4 Semiclassical description of the double-slit experiment

As we mentioned above, the dynamics described by the system (12), represents semiclassically the behavior of the quantum system under consideration, and thus it is constrained by Heisenberg's uncertainty (13). This relation allows us to establish initial conditions for effective variables ($G^{a,b}$). We can impose, for instance, that quantum variables saturate the lower bound in (13)

$$G_o^{2,0}G_o^{0,2} - (G_o^{1,1})^2 = \frac{\hbar^2}{4} \quad (13)$$

We propose an initial Gaussian state

$$\Psi_o = \frac{1}{(2\pi\sigma_o^2)^{1/4}} \exp \left(-\frac{(x - x_o)^2}{4\sigma_o^2} + i\frac{p_o}{\hbar}(x - x_o) \right). \quad (14)$$

from which quantum fluctuations $G_o^{2,0} = \Delta x_o^2$, $G_o^{0,2} = \Delta p_o^2$ and $G_o^{1,1} = \Delta x_o p_o$ can be obtained by computing usual expectation values, for example

$$G_o^{1,1} = \langle \Psi_o | (\hat{x} - x_o)(\hat{p} - p_o) | \Psi_o \rangle. \quad (15)$$

In this particular case, we obtain $G_o^{1,1} = 0$, and (13) becomes

$$G_o^{2,0}G_o^{0,2} = \frac{\hbar^2}{4} \quad (16)$$

For the two dimensional case we obtain two sets of initial conditions computed in a similar way, that is, (13) is replaced by

$$G_{io}^{2,0}G_{io}^{0,2} - (G_{io}^{1,1})^2 = \frac{\hbar^2}{4}, \quad i \in [x, y], \quad (17)$$

and the initial gaussian state is given by

$$\Psi_o(x, y) = \Psi_o(x)\Psi_o(y). \quad (18)$$

Once again $G_{io}^{1,1} = 0$.

We are interested in describing the evolution of the system in terms of canonical variables (s, p_s, U) . From (3) and (4) we obtain

$$G^{0,2} = \frac{1}{s^2}(U + p_s^2 s^2). \quad (19)$$

From $G_o^{1,1} = 0$ we see that $p_{s_o} = 0$ and (19) reduces to

$$G_o^{0,2} = \frac{U}{s_o^2}. \quad (20)$$

In the two dimensional regime, (20) is replaced by

$$G_{io}^{0,2} = \frac{U}{s_{io}^2}, \quad p_{s_{io}} = 0, \quad i \in [x, y]. \quad (21)$$

From these expressions we obtain initial values for canonical variables s_i .

4.1 Semiclassical trajectories

Equations (12) constitutes a nonlinear system of coupled differential equations, for which no analytical solution exists. Initial conditions for classical variables (x, y, p_x, p_y) can be fixed from the configuration of

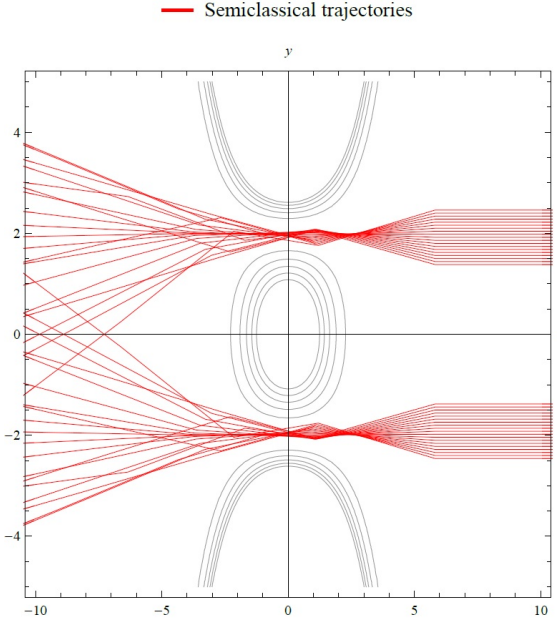


Figure 2: Semiclassical trajectories for the double-slit experiment.

the experiment, as in [8, 22]. These conditions are modified mainly by different experimental arrangements depending on the type of particles employed [4, 6, 22], the material used as the barrier [1], and the properties under study in the experiment [5]. This variety of configurations establish different initial

conditions, whose values change slightly from those in [3–6, 22]. We employ initial conditions for classical variables as in [6], and for canonical variables $(s_x, p_{sx}, s_y, p_{sy})$, as discussed in section 4, we set

$$\begin{aligned} x_o &= 400, & y_o &\in [-4, 4], & p_{xo} &= -5000, & p_{yo} &= 0, \\ p_{sxo} &= 0, & p_{sy} &= 0, & s_{xo} &= 0.2, & s_{yo} &= 0.2, & U &= 0.25 \end{aligned} \quad (22)$$

Feeding these data in (12) one can solve numerically. We show below several behaviors for particle evolution.

Semiclassical trajectories for individual particles crossing the potential barrier are shown in Fig. 2. Notice that some particles, coming from upper half of the barrier, can be detected in the lower half of the plane and vice versa. The recording screen is placed at $x = -350$.

Most particles are detected around the symmetry line, displaying the behavior shown in Fig. 4

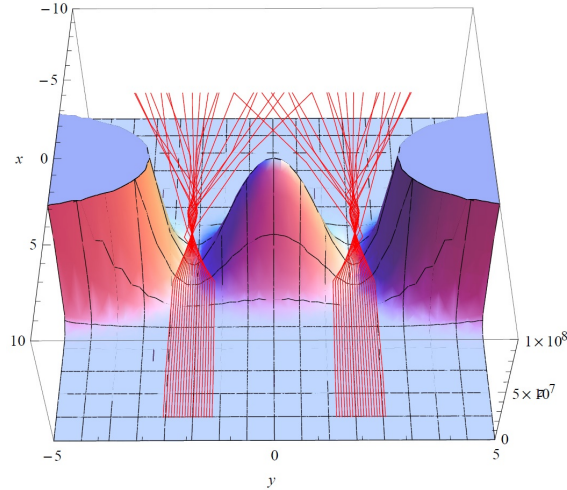


Figure 3: Semiclassical 3D trajectories for the double-slit potential with $E = 25 \cdot 10^6$

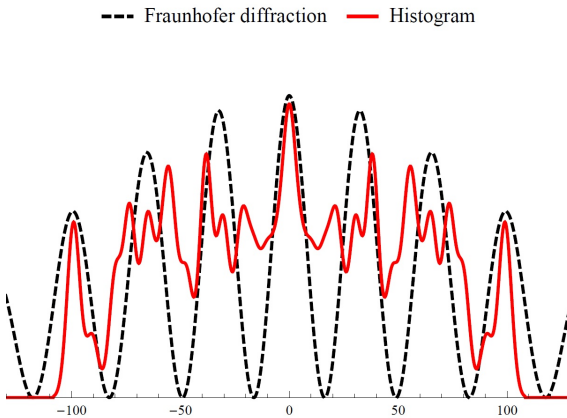


Figure 4: Frequency curve of particles arriving at $x = -350$ (red line), and the Fraunhofer diffraction pattern (black dashed line) which shows clearly that the maximum fringe is located where most of the lines in Fig. 2 are overlapped.

4.2 Trajectories with quantum dispersions and new insights

Momentous quantum mechanics allows obtaining of semiclassical trajectories, and it also provides a way to compute the evolution of dispersions (13). Quantum uncertainty must be taken into account, and thus the position of individual particles is computed in the following way

$$x(t) \pm s_x(t), \quad \text{and} \quad y(t) \pm s_y(t). \quad (23)$$

Several particle trajectories and their dispersions are plotted in Fig. 5, where the uncertainty belt is also shown (23). Uncertainty for crossing trajectories, as mentioned above, is shown in Fig. 6. In Fig.

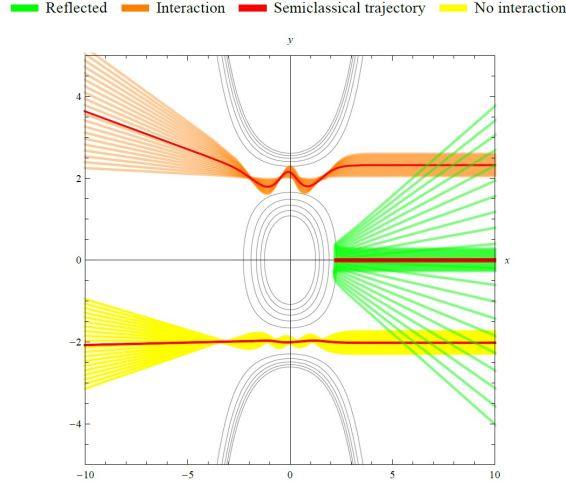


Figure 5: Trajectories in the double-slit experiment: particles being reflected (green area), particles strongly interacting with the potential (orange area), and particles with weak interaction (yellow area)

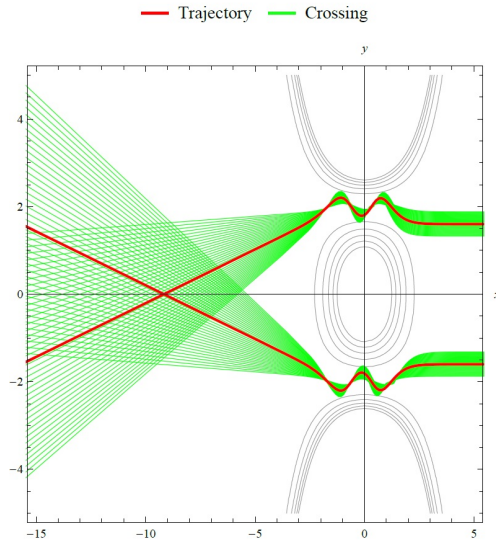


Figure 6: Quantum uncertainty (green area) for trajectories (red line), crossing after the barrier.

7, point particles display their wave behavior: one can see this as the overlapping of front waves coming out of the slits.

5 Discussion

There exist different explanations for the double-slit experiment in the literature. According to standard quantum mechanics, particles can cross both slits at the same time, even in a one-by-one setup [22]. However, this takes into account only the interference pattern displayed on the screen, it does not consider which slit the particle has crossed. Which-way experiments [2] attempt to determine that: one wishes to establish which slit the particle has crossed, and in some cases, particles coming from the upper half of the double slit can be recorded in the lower part of the screen, and vice versa [14].

There is no classical description for this. However, Bohmian mechanics, which offers a way to study quantum systems without abandoning classical concepts, such as trajectories, velocities, positions, may provide a way to explain exactly that. It is capable of reproducing the same statistical predictions as

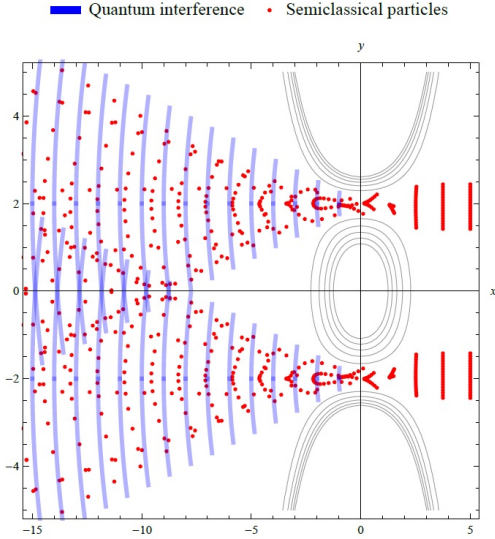


Figure 7: Particles (red dots) clustering in wavefronts (blue line).

standard quantum mechanics. However, trajectories in this scheme display what is called the "non-crossing rule" [11], which simply states that particles crossing the upper slit do not cross to the lower half of the screen, and vice versa. This behavior is in direct conflict with the results obtained in the experiments.

These features can be explained directly in our model. Particles arriving at the barrier interact with the potential, cross the slits and then follow semiclassical trajectories. Some of them remain in their half plane and others cross to the opposite side on the screen, as shown in figures 2,5,6,7. Our results are in no way classical, quantum dispersions are also dynamical and modify effectively the classical behavior of particles and their trajectories, as shown in Fig.6. This can be interpreted in the following way: at the barrier the dispersion get squeezed by interacting with the potential, this provokes a significant modification of their classical behavior through quantum back reaction, altering the original trajectory and allowing deflection to the opposite half plane in some cases. By considering the individual position of particles, we observe how their wave nature is reproduced by this effective dynamical evolution. In this picture, interference can be understood as particles clustering in a small region of space, behaving as if they were traveling on wave fronts, as shown in Fig. 7.

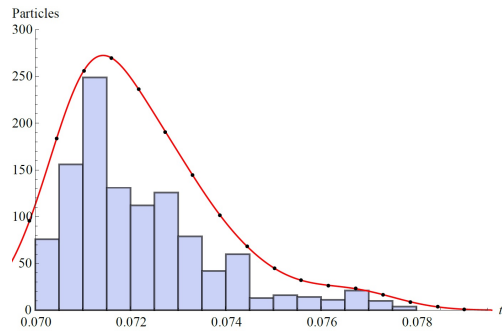


Figure 8: Time of arrival of particles to the screen located in $x = -350$.

Another interesting feature of our model, due to its semiclassical nature, is the possibility to analyze the time of arrival or flight time, in quantum systems [6]. For our double slit model we used similar initial conditions for classical and quantum variables to those used in actual experimental setups, but not so for initial velocities. We are able to obtain times of arrival for every configuration of our system, as shown in Fig.8, although, in order to get more experimentally interesting results, a more thorough analysis must be performed.

Our formulation can be employed in the study of complex quantum systems, such as the simulation of the double-slit experiment [23, 24], the double-slit quantum eraser [25], the study of semiclassical quantum billiards [26, 27], electron and neutron optical systems [28, 29], and several other applications.

References

- [1] E. J. S. Fonseca, P. H. Souto Ribeiro, S. Pádua, C. H. Monken, *Phys. Rev. A* **1999**, *60*, 1530.
- [2] J. Q. Quach, *Phys. Rev. A* **2017**, *95*, 042129.
- [3] M. W. Noel, C. R. Stroud, Jr., *Phys. Rev. Lett.* **1995**, *75*, 1252.
- [4] F. Shimizu, K. Shimizu, H. Takuma, *Phys. Rev. A* **1992**, *46*, R17.
- [5] F. Lindner, M. G. Schätzel, H. Walther, A. Baltuška, E. Goulielmakis, F. Krausz, D. B. Milošević, D. Bauer, W. Becker, G. G. Paulus, *Phys. Rev. Lett.* **2005**, *95*, 040401.
- [6] H. Nitta, T. Kudo, *Phys. Rev. A* **2008**, *77*, 014102.
- [7] D. Bohm, *Phys. Rev.* **1952**, *85*, 166.
- [8] W. P. Schleich, M. Freyberger, M. S. Zubairy, *Phys. Rev. A* **2013**, *87*, 014102.
- [9] B. Braverman, C. Simon, *Phys. Rev. Lett.* **2013**, *110*, 060406.
- [10] P. R. Holland, Cambridge University Press, Cambridge, **1993**.
- [11] A. B. Nassar, S. Miret-Artés, *Historical and Introductory Account of Bohmian Mechanics*, Springer International Publishing, Cham, **2017**.
- [12] P. Ghose, A. Majumdar, S. Guha, J. Sau, *Phys. Lett. A* **2001**, *290*, 205.
- [13] G. Grössing, S. Fussy, J. Mesa Pascasio, H. Schwabl, *Ann. Phys.* **2012**, *327*, 421.
- [14] B.-G. Englert, M. O. Scully, G. Süssmann, H. Walther, *Zeitschrift für Naturforschung A* **1992**, *47*, 1175.
- [15] M. Bojowald, A. Skirzewski, *Rev. Math. Phys.* **2006**, *18*, 713.
- [16] B. Baytaş, M. Bojowald, S. Crowe, *Phys. Rev. A* **2019**, *99*, 042114.
- [17] B. Baytaş, M. Bojowald, S. Crowe, *Phys. Rev. A* **2018**, *98*, 063417.
- [18] H. H. Hernández, G. Chacón-Acosta, *AIP Conf. Proc.* **2012**, *1473*, 168.
- [19] L. Aragón-Muñoz, G. Chacón-Acosta, H. Hernandez-Hernandez, *Int. J. Mod. Phys. B* **2020**, *34*, 2050271.
- [20] M. Bojowald, D. Brizuela, H. H. Hernández, M. J. Koop, H. A. Morales-Técotl, *Phys. Rev. D* **2011**, *84*, 043514.
- [21] O. V. Prezhdo, *Theor. Chem. Acc.* **2006**, *116*, 206.
- [22] A. Tonomura, J. Endo, T. Matsuda, T. Kawasaki, H. Ezawa, *Amer. J. Phys.* **1989**, *57*, 117.
- [23] M. Gondran, A. Gondran, *Amer. J. Phys.* **2005**, *73*, 507.
- [24] A. Zeilinger, R. Gähler, C. G. Shull, W. Treimer, W. Mampe, *Rev. Mod. Phys.* **1988**, *60*, 1067.
- [25] S. P. Walborn, M. O. Terra Cunha, S. Pádua, C. H. Monken, *Phys. Rev. A* **2002**, *65*, 033818.
- [26] G. Carlo, E. Vergini, A. J. Fendrik, *Phys. Rev. E* **1998**, *57*, 5397.
- [27] O. de Alcantara Bonfim, J. Florencio, F. Sá Barreto, *Phys. Lett. A* **2000**, *277*, 129.
- [28] W. P. Schleich in John Wiley & Sons, Ltd, New York, **2001**.
- [29] M. O. Scully, M. S. Zubairy, *Quantum Optics*, Cambridge University Press, **1997**.